

Journal of Materials Chemistry B

Accepted Manuscript



This is an *Accepted Manuscript*, which has been through the Royal Society of Chemistry peer review process and has been accepted for publication.

Accepted Manuscripts are published online shortly after acceptance, before technical editing, formatting and proof reading. Using this free service, authors can make their results available to the community, in citable form, before we publish the edited article. We will replace this *Accepted Manuscript* with the edited and formatted *Advance Article* as soon as it is available.

You can find more information about *Accepted Manuscripts* in the [Information for Authors](#).

Please note that technical editing may introduce minor changes to the text and/or graphics, which may alter content. The journal's standard [Terms & Conditions](#) and the [Ethical guidelines](#) still apply. In no event shall the Royal Society of Chemistry be held responsible for any errors or omissions in this *Accepted Manuscript* or any consequences arising from the use of any information it contains.

PAPER

A Lipopolysaccharide Binding Heteromultivalent Dendrimer NanoplatforM for Gram Negative Cell Targeting

Cite this: DOI: 10.1039/x0xx00000x

Received 00th January 2012,

Accepted 00th January 2012

DOI: 10.1039/x0xx00000x

www.rsc.org/

Pamela T. Wong,^{a, b} Shengzhuang Tang,^{a, b} Kenny Tang,^a Alexa Coulter,^a Jhinda Mukherjee,^{a, b} Kristina Gam,^a James R. Baker Jr.,^{a, b} and Seok Ki Choi^{a, b, *}

We report on the practicality of a heteromultivalent design strategy for a nanoplatforM that targets lipopolysaccharide molecules (LPS) present on the surface of Gram-negative bacteria. This design is based on the conjugation of a poly(amido amine) (PAMAM) dendrimer with two types of ligands, each having distinct affinities: i) polymyxin B (PMB) as a primary high affinity ligand; ii) a PMB-mimicking dendritic branch as an auxiliary low affinity ligand. Co-conjugation of these two ligands maximizes the efficiency of the primary ligand even when the primary ligand is present at a low valency on the nanoplatforM (mean $n_{\text{PMB}} \approx 1$). By performing surface plasmon resonance studies using a LPS-immobilized cell wall model, we identified an ethanolamine (EA)-terminated branch as the auxiliary ligand that promotes binding avidity via heteromultivalent association. PMB conjugation of the dendrimer with excess EA branches led to LPS avidity two orders of magnitude greater than unconjugated PMB. Such tight binding observed by SPR corresponded well with adsorption to *E. coli* cells and with potent bactericidal activity *in vitro*.

1 Introduction

Gram-negative bacteria are causative agents for serious infections and have the potential to pose a biological threat to public safety.¹⁻³ Rapid detection and identification of causative pathogens are of utmost importance for effective treatment of these infectious diseases.^{1, 4} Current diagnostic methods for bacterial infections have certain limitations in their speed and sensitivity,^{1, 3} and there are growing demands to develop novel strategies and therapeutic methods for rapid detection and effective treatment.⁵⁻⁷ Recent advances made in nanotechnology provide promising tools and strategies for bacteria-specific detection and activity.⁸⁻¹⁷ Such strategies vary depending on the type of nanoscale particles (NPs), but all attempt to selectively target bacterial cells by multivalent

conjugation with ligands such as mannoside,¹² mannose-binding lectin,¹⁷ Zn-dipicolylamine (DPA)¹¹ and antimicrobial agents (vancomycin,^{9, 13, 14, 16} polymyxin B (PMB),^{15, 25, 26} cationic antimicrobial peptides^{18, 19}). This multivalent design allows much tighter and more selective NP adsorption to the target surface than monovalent binding.²⁰⁻²²

Multivalent design of NPs specific for Gram-positive bacterial cells has been well established by use of vancomycin²³ due to its specific affinity for the (D)-Ala-(D)-Ala peptide ($K_D \approx 10^{-6} \text{ M}$),^{16, 24} a cell wall precursor embedded in the peptidoglycan (PG) layer.^{9, 13, 14, 16, 25} In contrast, strategies for targeting Gram-negative cells are less explored, resulting in fewer NP systems including those based on magnetic NP,¹¹ poly(acrylamide)¹⁵ and human globulins,^{26, 27} each conjugated with PMB^{15, 26, 27} or Zn-DPA,¹¹ as the ligand for bacterial capture¹¹ or antiendotoxin agents.^{26, 27} However, in each of these systems, quantitative evaluation of binding avidity has not been performed and thus multivalent design parameters important for optimizing the targeting systems remain unknown.

In this communication, we describe the practical advantages of heteromultivalency²⁸⁻³¹ in the design of multivalent NPs that target lipopolysaccharide (LPS) molecules presented on the surface of a Gram-negative cell (Fig. 1). LPS molecules

^a Michigan Nanotechnology Institute for Medicine and Biological Sciences, University of Michigan, Ann Arbor, Michigan 48109, United States

^b Department of Internal Medicine, University of Michigan, Ann Arbor, Michigan 48109, United States

* Corresponding author: skchoi@umich.edu

† Electronic Supplementary Information (ESI) available: Experimental details for conjugate synthesis, SPR, confocal microscopic study, antimicrobial assay and release study. See DOI: 10.1039/c000000x/

represent a preferred target because of its physical accessibility, high surface density ($0.7\text{--}1.0 \times 10^5$ molecules/ μm^2)³² and the availability of high affinity ligands such as PMB^{33–35} ($K_D \approx 4\text{--}6.4 \times 10^{-7}$ M^{36, 37}). As a member of the cationic class of peptide antibiotics, PMB is highly effective at killing Gram(–) bacterial cells due to its tight binding to the LPS molecule, which leads to cell wall disruption and lysis. However, PMB causes nephrotoxicity because of its preferential uptake and accumulation in renal cells.³⁸ Thus, despite its ability to target bacterial LPS, the systemic toxicity of PMB makes it preferable to limit the amount of PMB conjugated to dendrimer. However, PMB conjugation at a low valency can compromise the binding avidity of the resulting nanoconjugate. Here, we address such a contradictory design issue by exploring a heteromultivalent approach^{28–31} that enables to achieve high avidity binding to LPS with conjugation of only one or two PMB ligands with the support with a large excess of a low affinity auxiliary ligand.

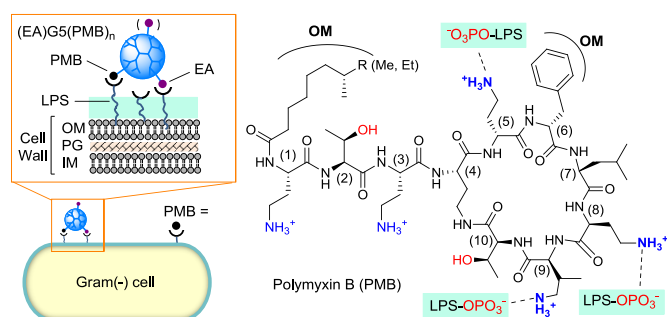


Fig. 1 A schematic model for surface adsorption of heteromultivalent G5 PAMAM dendrimer conjugated with PMB and excess ethanolamine (EA) branches to a Gram-negative bacterium (left). Structure of polymyxin B (PMB) (B_1 : R = Me; B_2 : R = Et) and specific epitopes involved in interaction with lipopolysaccharide (LPS) presented on the outer membrane (OM) (right). PG = peptidoglycan layer; IM = inner membrane.

2 Experimental section

2.1 Materials and analytical methods

Unless noted otherwise, all reagents and solvents were purchased from Sigma-Aldrich and used as received. These include lipopolysaccharides (from *Escherichia coli* 0127-B8), ciprofloxacin ($\geq 98\%$), vancomycin hydrochloride hydrate, epibromohydrin, glycidol, ethanolamine and fluorescein 5(6)-isothiocyanate (FITC; purity $\sim 90\%$). Polymyxin B sulfate (>6500 IU/mg) was purchased from AK Scientific, Inc. HBS-EP buffer solution and sensor chip CM5 for SPR studies were purchased from GE Healthcare. A fifth generation (G5) poly(amido amine) (PAMAM) dendrimer was purchased as a solution in methanol (17.5 % (w/w); Dendritech, Inc.), and purified prior to use by dialysis (MWCO 10 kDa) against deionized water as described elsewhere.³⁹ G5 dendrimer modified with glutaric acid, G5(GA), was prepared as described elsewhere.^{40, 41}

All ^1H NMR spectra were acquired with a Varian NMR spectrometer (500 MHz) at 297.3 K (± 0.2) using standard pulse sequences and in a deuterated solvent as noted in each

spectrum. Chemical shift values were recorded in a δ (ppm) unit with an internal standard (2,2-dimethyl-2-silapentane-5-sulfonate sodium salt, DSS) as $\delta = 0.00$ ppm. UV-vis spectra were recorded with a Perkin Elmer Lambda 25 spectrophotometer. Molecular weights (M_r) of G5 PAMAM dendrimer and its conjugates were determined by matrix assisted laser desorption ionization time-of-flight mass spectrometry (MALDI-TOF MS) with a Waters TOFSpec-2E spectrometer.

Ultra-performance liquid chromatography (UPLC) was performed on a Waters Acquity Peptide Mapping System equipped with a Waters photodiode array detector. Each sample was prepared at the concentration of $0.1\text{--}1.0$ mg mL^{-1} (in water or 20% aq acetonitrile) and analyzed by running on a C4 BEH column (100×2.1 mm, 300 Å) using a method previously developed: flow rate = 0.2 mL min^{-1} ; a linear gradient method starting with an initial mobile phase composition 99:1 (v/v) water/acetonitrile with TFA (0.1% v/v) (eluent A and B,

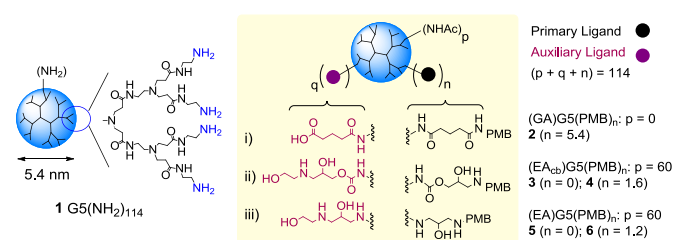


Fig. 2 Structural features of 1 G5(NH₂) and three types of linker chemistry (i–iii) used for preparing heteromultivalent conjugates G5(PMB)_n, 2–6, each terminated with excess glutaric acid (GA) or ethanol amine (EA) branches in combination with polymyxin B (PMB) at low valency.

respectively). The gradient was 1% B (0–1.4 min), linear increase to 80% B (1.4–13.4 min), linear decrease to 50% B (13.4–13.8 min), linear decrease to 1% B (13.8–14.4 min) and 1% B (14.4–18 min).

Gel permeation chromatography (GPC) was performed in an Alliance Waters 2695 separation module. Signal intensity of eluted dendrimer particles was measured at two detection modes: i) a Wyatt HELEOS Multi Angle Laser Light Scattering detector; ii) an Optilab rEX differential refractometer (Wyatt Technology Corporation). Each GPC sample was prepared at 3–5 mg/mL in an elution buffer (0.1 M citric acid, pH 2.7–2.76 with 5 ppm Kathon II). Data analysis was performed with Astra 5.3.14 software (Wyatt Technology Corporation) to extract molecular weights (weight-average molecular weight (M_w), number-average molecular weight (M_n)) and polydispersity index ($\text{PDI} = M_w/M_n$).

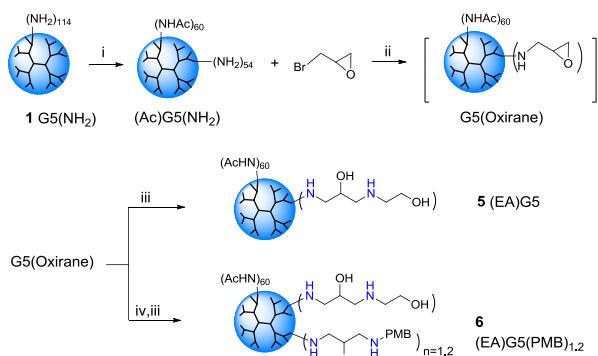
The charge and size distribution of dendrimer conjugates were determined by measurement of zeta potential (ZP) and dynamic light scattering (DLS) on a Zetasizer Nano ZS (Malvern).^{42, 43} Each dendrimer was prepared at 0.05 mg/mL in HEPES buffer (1 mM, pH 7), and the zeta sizing experiments were performed at room temperature.

2.2 Representative synthesis of G5 dendrimer conjugates

Three types of linker chemistries were employed for conjugation of PMB to a fifth generation (G5) PAMAM dendrimer, and five dendrimer conjugates **2–6** were prepared (Fig. 2, Scheme 1). Below are representative methods for synthesis of conjugate **5** and **6** while synthetic procedures for remaining conjugates **2–4** are provided in details in Supporting Information (Schemes S1–S3).

G5(OXIRANE). Preparation of G5(Oxirane). To a stirred solution of **1** G5(NH₂) (150 mg, 5.43 μmol) in methanol (20 mL) was added DIPEA (56.8 μL, 0.326 mmol) and Ac₂O (30.8 μL, 0.326 mmol) in a dropwise manner as a neat liquid. After vigorous stirring at room temp for 2 min, epibromohydrin (18.6 μL, 0.217 mmol) was added to the dendrimer treated with Ac₂O. The reaction mixture was stirred at room temp for 9 h to generate a reactive conjugate G5(Oxirane). This solution (20 mL) was divided into two lots (13.5 mL, 6.5 mL each) and each lot was used without further treatment immediately for a next conjugation reaction.

5 (EA)G5. To G5(Oxirane) (6.5 mL lot) was added a NaOH solution (1.0 M, 36 μL) and ethanolamine (44 μL, 0.725 mmol). The resulting mixture was shaken at 45°C for 12 h, and concentrated *in vacuo*. The residue was dissolved in water (5 mL), loaded into a membrane dialysis tubing (MWCO 10 kDa) and dialyzed against water (4 L × 3) for 2 days. After



Scheme 1. Synthesis of dendrimer conjugates **5**, **6**. *Reagents and conditions:* i) Ac₂O (60 mol equiv), DIPEA, MeOH, room temp; ii) epibromohydrin (40 mol equiv), 9 h, room temp; iii) ethanolamine (200 mol equiv), 45°C, 12 h; iv) polymyxin B sulfate (10 mol equiv), NaOH (50 mol equiv), H₂O, MeOH, 45°C, 20 h.

lyophilization of the dialyzed solution, the conjugate **5** (EA)G5 was obtained as white solid (54 mg). The homogeneity of conjugate **5** was analyzed by a HPLC method (Fig. S2): $t_r = 6.9$ min; polymer purity 96%. GPC (Fig. S1): $M_n = 27,900$ gmol⁻¹, PDI = 1.33. MALDI-TOF mass spectrometry (m/z ; gmol⁻¹; Fig. S3): 29,800. UV-vis (PBS, pH 7.4; Fig. S4): $\lambda_{max} = 282$ nm ($\epsilon = 2,390$ M⁻¹cm⁻¹). ¹H NMR (500 MHz, DMSO-*d*₆; Fig. S7): 8.3–7.8 (br m), 4.48 (weak br), 4.15 (weak m), 3.7–3.3 (strong m), 3.2–2.9 (strong s), 2.8–2.6 (strong s), 2.55 (strong s), 2.5–2.4 (m), 2.3–2.1 (strong s), 1.85 (s), 1.8 (strong s) ppm.

6 (EA)G5(PMB)_n. To G5(Oxirane) (13.5 mL lot) was added a solution of polymyxin B sulfate (50 mg, 36.2 μmol) dissolved in 1.0 mL of water, and followed by the addition of a NaOH

solution (1 M, 0.181 mL). The mixture was shaken at 45°C for 20 h, and ethanolamine (44 μL, 0.725 mmol) was added. The final mixture was shaken at 45°C for 12 h and concentrated *in vacuo*. The residue was dissolved in water (10 mL) and dialyzed (MWCO 10 kDa; 4 L of water × 3) for 2 days. After lyophilization of the dialyzed solution, the conjugate **6** (EA)G5(PMB)_n was obtained as white solid (104 mg). The homogeneity of conjugate **6** was analyzed by a HPLC method (Fig. S2): $t_r = 6.9$ min, free PMB undetectable, polymer purity ≥93%. GPC (Fig. S1): $M_n = 27,500$ gmol⁻¹, PDI = 1.26. MALDI-TOF mass spectrometry (m/z ; gmol⁻¹; Fig. S3): 30,200. UV-vis (PBS, pH 7.4; Fig. S4): $\lambda_{max} = 281$ nm ($\epsilon = 2,900$ M⁻¹cm⁻¹). ¹H NMR (500 MHz, DMSO-*d*₆; Fig. S7): 8.3–7.8 (br m), 7.55–7.4 (weak br), 7.3–7.1 (weak br), 4.48 (weak br), 4.15 (weak br), 3.8–3.3 (strong s), 3.2–2.9 (strong m), 2.8–2.6 (strong s), 2.55–2.4 (strong m), 2.3–2.1 (strong s), 1.8 (strong s), 1.45 (weak br), 1.25 (weak br), 1.15–1.0 (weak m), 0.8 (weak br) ppm. A NMR integration method was used to determine the PMB valency (n) by comparison of (D)-Phe (PMB) signal (δ 7.3–7.1 ppm) to a reference group of NHAc at δ 1.8 ppm (60 Ac residues per dendrimer), yielding $n = 1.2$ (± 0.3).

2.3 Surface Plasmon Resonance (SPR) Spectroscopy^{16, 43–45}

SPR experiments were performed on a Biacore® X instrument (Pharmacia Biosensor, AB) using a CM5 sensor chip immobilized with LPS (Scheme S4; details for LPS immobilization given in Supporting Information). SPR study was carried out by injection (50 μL) of analyte solutions, each prepared in HBS-EP buffer and through serial dilutions. The analyte run at a flow rate of 30 μL/min. At the end of each dissociation phase ($t > 600$ s), the chip surface was regenerated by treatment with 10 μL of 10 mM glycine-HCl (pH 2.5).

For SPR data analysis, the contribution of non-specific adsorption was corrected by subtraction of the sensorgram in flow cell 1 (RU₁) by the reference sensorgram in flow cell 2; RU₂: ΔRU (corrected) = RU₁ – RU₂. Dissociation constant K_D was determined by extraction of two kinetic parameters—association (on) rate constant (k_{on}) and dissociation (off) rate constant (k_{off}). Global fitting analysis was performed for each corrected sensorgram to the Langmuir adsorption isotherm to determine k_{off} , k_{on} and K_D ($= k_{off} \div k_{on}$).⁴⁶ The K_D value was obtained as a mean value from four or more independent measurements ($n \geq 4$), each calculated from a pair of the two associated rate constants.

2.4 Mass spectrometry for release kinetics

LCMS/MS analysis was performed with a Waters TQ detector mass spectrometer equipped with Waters Acquity UPLC system using on an ODS column (XBridge BEH C18 2.5 μm; 2.1 × 50 mm, Waters) as described elsewhere.⁴⁷ The method for elution gradient begins with 90 % aqueous ammonium formate (10 mM; A)/10 % aqueous acetonitrile (B) and ends with 50/50 (A/B) over the course of 5 min with a flow rate of 0.5 ml/min and at a column temperature of 40°C. A calibration curve for ciprofloxacin was generated by analysis of each of its aqueous

standard solutions (50–250 nM) in triplicate. Ciprofloxacin was detected at $t_R = 2.64$ min and its area under curve (AUC) was quantified by focusing this molecular species. The limit of detection (LOD) determined for ciprofloxacin was in the range of ≥ 50 –70 nM.

The ciprofloxacin alone control or each of the complex solutions was transferred to a Float-A-lyser[®] membrane tube (Amicon; MWCO 3000–5000), and was placed in a beaker containing deionized water (300 mL). The water in the beaker was magnetically stirred and a series of aliquots, each 0.2 mL, were taken out at specific time points (0, 5 min, 10, 15, 30 min, 1 h, 2, 3, 6, 21, and 24 h). After each aliquoting, a same volume of deionized water (0.2 ml) was replenished into the beaker to maintain the same volume of water outside. These aliquots were analyzed by LCMS/MS spectrometry, and the cumulative concentrations of ciprofloxacin released and diffused into the water outside were determined relative to a calibration curve prepared by standard ciprofloxacin solutions. Details for preparation of a ciprofloxacin alone control, and ciprofloxacin-dendrimer complexes are described in Supporting Information.

2.5 Confocal microscopy^{16, 43, 48}

E. Coli cells (XL-1) were scraped from a frozen stock with a sterile loop, inoculated into 8 mL of LB, and incubated in a 37°C shaker o/n, and the CFU/mL was determined. For each treatment condition, 2.5×10^5 CFU *E. Coli* was spun down at 9,000 rpm for 10 min in a microfuge, and washed twice with PBS. Cells were resuspended in a total volume of 250 μ L of dendrimer conjugate in PBS, giving final concentrations of 1×10^6 CFU/mL *E. Coli*, and 2.5 mg/mL conjugate. Samples were vortexed and incubated at room temp on an orbital shaker for 30 min. Cells were spun down at 9,000 rpm for 10 min, and washed twice with PBS. Cells were fixed in 4% paraformaldehyde for 10 min at room temp, and rinsed with PBS. Cells were resuspended in and stained with 1 μ M of Syto 59 (Life Technologies) for 10 min at room temp in PBS, and then washed twice with PBS. Stained cells were resuspended in 50 μ L of PBS, dropped onto a coverglass slide and allowed to dry before mounting in ProLong Gold (Life Technologies). Images were collected on a Leica inverted SP5X confocal microscope (Leica Microsystems) and the fluorescence was measured for FITC (ex = 488 nm, em = 520–560 nm) and Syto 59 (ex = 622, em = 640–660 nm) at 63 \times magnification.

2.6 Turbidity assay¹⁶

Five mL of bacterial cultures of *E. Coli* (XL-1) cells were grown overnight in a 37°C shaker in LB. The CFU/mL of the culture was determined, and 1×10^6 CFU of cells were added to each well of a 96 well plate in LB. Serial dilutions of the dendrimer conjugates were performed in LB and added to the cells over a final dendrimer or free drug concentration range of 20 nM–2.5 μ M. An initial baseline reading of turbidity was taken by measuring the absorbance at 650 nm in a plate reader spectrophotometer Epoch (BioTek). Cells were incubated for 24 h at 37°C, and the absorbance at 650 nm was measured.

Baseline turbidity at 0 h was subtracted from the 24 h turbidity reading to yield the final Abs 650 nm value as shown.

3 Results and discussion

In this heteromultivalent approach, we use two different types of ligands, each binding an identical LPS target though with variable affinities. PMB was used as a primary ligand to LPS due to its high affinity. Here, it was conjugated to a fifth generation (G5) PAMAM dendrimer ($d = 5.4$ nm)⁴⁹ as a scaffold for heteromultivalent NP design. The structure of this dendrimer **1** G5(NH₂)_n has unique features that make it optimal for this purpose because of its conformational flexibility and large number of terminal branches ($n_{\text{theor}} = 128$),⁴⁹ each amenable for PMB conjugation or modification to an auxiliary ligand mimicking the PMB molecule (Fig. 2). We hypothesized that such ligand mimics to PMB may be generated through chemical modification of dendritic amines oriented in a spatial proximity analogous to the configuration of key functional groups of PMB responsible for LPS binding that occurs through electrostatic attraction and polar contact interactions.^{34, 35}

3.1 Design and synthesis of dendrimer conjugates

In this study, we define a heteromultivalent system as the dendrimer conjugated with PMB as well as modified with an LPS-binding auxiliary ligand. However, the PMB-conjugated dendrimer modified with a linker branch that lacks LPS binding is defined otherwise as a functionally homomultivalent system. Three types of linker chemistries were considered for PMB conjugation and for generating excess molecular copies of a potential auxiliary ligand branch (Fig. 2; Schemes S1–S3). In this approach, we screened three types of bifunctional molecules with different linker chemistries which included glutaric acid (GA), glycidol and epibromohydrin. Each of these linkers differs in the manner in which they are cross-linked to the dendrimer and to PMB. The glutarate molecule provides two carboxylate groups, each amenable for coupling to the dendrimer and PMB via a neutral amide bond, or potentially serving as an anionic auxiliary ligand if left unconjugated. Glycidol has a primary alcohol that can be used for coupling to the dendrimer via a neutral carbamate bond. In addition, it has an epoxide ring at the other end which can undergo a cross-linking reaction with a PMB or auxiliary ligand (ethanolamine) molecule with retention of cationic amine functionality. Epibromohydrin allows cross-linking with retention of the cationic amine functionality at both of its ends.

First, an amide linker was used for the EDC-based covalent coupling of PMB with a glutaric acid-modified G5 dendrimer (GA)G5⁴⁸ ($M_r = 40200$ g mol⁻¹, PDI = $M_w/M_n = 1.046$; see Supporting Information) to give conjugate **2** (GA)G5(PMB)_n ($M_r = 46,400$ g mol⁻¹) with a Poissonian distribution of PMB valency ($n_{\text{mean}} = 5.4 \pm 0.51$, $n_{\text{median}} = 5.5$; Table S1). Second, partial acetylation of **1** G5(NH₂) was performed to give (Ac)₆₀G5(NH₂), and subsequently carbamate (cb) was used for further modification with EA and PMB conjugation, resulting in two conjugates (EA_{cb})G5 **3** ($M_r = 31,900$ g mol⁻¹) and (EA_{cb})G5(PMB)_n **4** ($M_r = 32,100$ g mol⁻¹; $n_{\text{mean}} = 1.6 \pm 0.10$, $n_{\text{median}} = 2.5$). Third, amine functionality of the G5 dendrimer

was used to maintain a cationic charge at the dendritic terminus, yielding two conjugates (EA)G5 **5** ($M_r = 29,800 \text{ g mol}^{-1}$) and **6** ($M_r = 30,200 \text{ g mol}^{-1}$; $n_{\text{mean}} = 1.2 \pm 0.33$, $n_{\text{median}} = 2$).

We determined the physical properties of these dendrimer conjugates including their charge and size distribution as summarized in Table S2. The ZP values for **1** G5(NH₂)₅, **2** (GA)G5(PMB)_{5,4}, **3** (EA_{cb})G5, **4** (EA_{cb})G5(PMB)_{1,6}, **5** (EA)G5 and **6** (EA)G5(PMB)_{1,2} are 12.9 ± 5.6 , -25.5 ± 3.9 , 12.1 ± 6.8 , 10.5 ± 5.2 , 19.1 ± 6.3 , and $20.3 \pm 3.9 \text{ mV}$, respectively. Thus, each of these dendrimers is positively charged except **2** which is negatively charged. This charge difference is attributed to a large number of anionic carboxylate residues present on the surface of **2** (~103 GA per dendrimer). The carbamate-linked dendrimers **3**, **4** are less cationic than unmodified G5(NH₂), which is consistent with their structural features in which each of them is partially neutralized with NHAc before modification with cationic ethanolamine and PMB residues (Fig. 2). On the other hand, two other dendrimers **5**, **6** in a different series are more cationic than **3** and **4**. We believe that unlike the carbamate linkage used for **3**, **4**, the amine linkage for **5**, **6** allows the maintenance of a cationic charge at the site of cross-linking with ethanolamine and PMB.

Particle sizes determined by DLS for these dendrimers are 7.1 (**1**), 10.2 (**2**), 9.4 (**3**), 5.3 (**4**), 6.0 (**5**) and 6.1 nm (**6**). Here each size refers to a hydrodynamic diameter, and is thus larger than the theoretical size of unmodified dendrimer **1** (5.4 nm⁴⁹). Further size variation observed here appears to be related to the surface modification and charge state.

3.2 SPR binding study

The binding avidity of these dendrimers to the bacterial surface was evaluated by surface plasmon resonance (SPR) spectroscopy in a cell wall model for Gram-negative cells prepared by immobilization of LPS on the chip surface. PMB showed dose-dependent binding sensorgrams (Fig. S8) and Langmuir fitting analysis⁴⁶ performed for each sensorgram provided a K_D value of $1.5 \times 10^{-7} \text{ M}$ (Table 1). This monovalent affinity value is in close agreement with the values determined by other biophysical methods ($K_D = 4\text{--}6.4 \times 10^{-7} \text{ M}$),^{36, 37} demonstrating the susceptibility of the immobilized LPS to PMB binding. (GA)G5(PMB)_n **2** showed only a small response ($\Delta\text{RU} \leq 5$ at 11 μM ; Fig. S8) despite its moderately high PMB valency ($n_{\text{mean}} = 5.4$). This lack of strong adsorption may be attributable to the high density of negatively charged LPS (phosphate) groups on the chip surface that exert a repulsive force upon approach of this fully negatively charged dendrimer. (EA_{cb})G5 **3**, which did not have PMB attached, did not show any response while **4**, an equivalent dendrimer with PMB attached at a low valency ($n_{\text{mean}} = 1.6$), showed a relatively moderate level of adsorption and a K_D value of $8.8 \times 10^{-8} \text{ M}$, an avidity value that provides a small multivalent enhancement (β) factor of 1.7 over PMB. The SPR data suggest that the glutarate or carbamate-linked branches play no role as the auxiliary ligand, and thus the conjugates **2** and **4**, each presenting PMB attached through these linker types, bind according to a homomultivalent mechanism.

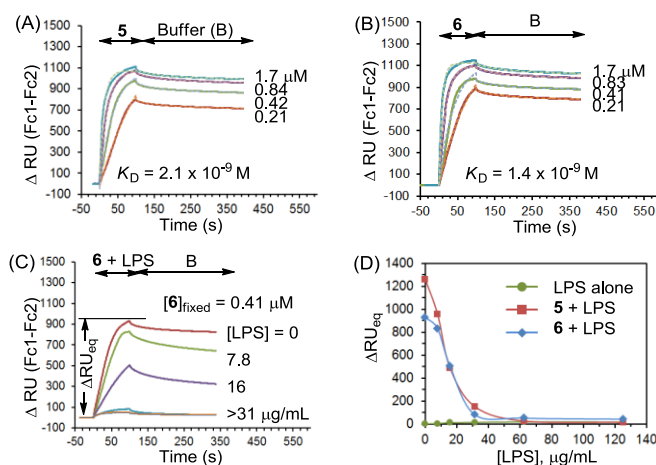


Fig. 3 (A–C) SPR sensorgrams for the binding kinetics of dendrimers to an LPS-immobilized CM5 sensor chip surface. (A) **5** (EA)G5; (B) **6** (EA)G5(PMB)_{1,2}. Solid lines (experimental); dotted lines (simulated global fits); (C, D) Competitive inhibition of dendrimer adsorption by LPS, and plot of $\Delta\text{RU}_{\text{eq}}$ vs [LPS].

Table 1. Kinetic rate constants and K_D values for binding of polymyxin B (PMB) and G5(PMB)_n 4–6 to the bacterial cell wall model determined by surface plasmon resonance spectroscopy.

Analyte	$k_{\text{on}} (\text{M}^{-1}\text{s}^{-1}) \times 10^{-4}$	$k_{\text{off}} (\text{s}^{-1}) \times 10^5$	$K_D (\text{M}),^a \text{ nM}$	β^b
PMB	5.9 (± 4.4)	400 (± 250)	150 (± 68)	1
4	3.5 (± 2.3)	400 (± 350)	88 (± 59)	1.7 (1.1 ^c)
5	4.9 (± 1.3)	9.9 (± 1.6)	2.1 (± 0.66)	71
6	6.5 (± 0.63)	8.9 (± 1.7)	1.4 (± 0.38)	107 (89 ^c)

^a $K_D = k_{\text{off}}/k_{\text{on}}$ ($\pm \text{SD}$) ($n = 5$). ^b $\beta = \text{Multivalent binding enhancement} = K_D^{\text{PMB}} / K_D^{\text{dendrimer}}$. ^c Valency-corrected value = β / n .

The highest dendrimer adsorption was observed for conjugates **5** and **6** (EA)G5(PMB)_n ($n_{\text{mean}} = 0, 1.2$) which present excess EA molecules attached to branches extended through an amine linkage (Fig. 3). Each conjugate shows an extremely slow dissociation rate ($k_{\text{off}} = 8.9\text{--}9.9 \times 10^{-5} \text{ s}^{-1}$) as reported for numerous other multivalent systems as a hallmark of tight multivalent binding.^{20–22} The K_D values of conjugates **5** and **6** are 2.1 and $1.4 \times 10^{-9} \text{ M}$, respectively, corresponding to an avidity enhancement of two orders of magnitude ($\beta = 71\text{--}107$) relative to PMB. We investigated whether such tight binding by **5** and **6** is specific to LPS immobilized on the surface by using a ligand competition assay in which free LPS is premixed with the conjugate prior to injection. As shown in Fig. 3C and Fig. S9, the addition of LPS to each conjugate led to a decrease in dendrimer adsorption as a function of LPS concentration, giving a sigmoidal curve. These results are supportive of the specificity of the cell wall model for LPS-targeted dendrimer adsorption. The high avidity displayed by **5** that lacks the PMB ligand strongly suggests the importance of the amine functionality used for linking an EA residue as an auxiliary ligand. Interestingly, use of other functionalities for ligand conjugation and/or attaching EA residues led to lack of such tight adsorption as illustrated by **2** and **3**.

3.3 Confocal microscopy

We next determined whether those conjugates **4–6** that bound to the model surface adsorb to live Gram-negative cells. We treated *Escherichia coli* (XL-1) with fluorescein 5(6)-isothiocyanate (FITC)-labelled conjugates and performed confocal fluorescence microscopy (Fig. 4). Images of the *E. coli* cells treated with each of these conjugates showed intense punctate areas of fluorescence attributable to the conjugate adsorbed to the cell wall. Some of the images show aggregates of *E. coli* cells which are believed to be formed by a mechanism of multivalent crosslinking between multiple dendrimer particles and *E. coli* cells as observed similarly in *Staphylococcus aureus* by vancomycin-conjugated

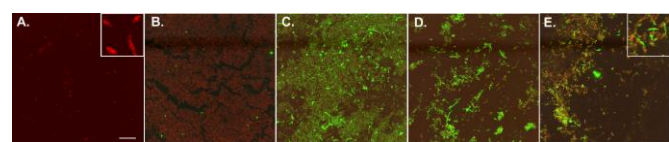


Fig. 4 Confocal fluorescence images of *E. coli* cells untreated (A) and treated with FITC-labelled dendrimers (green) (GA)G5(FI)₂ (B), **4** (EA_{cb})G5(PMB)_{1.6}(FI)_{1.3} (C), **5** (EA)G5(FI)_{0.6} (D) and **6** (EA)G5(PMB)_{1.2}(FI)_{1.5} (E). *E. coli* (A) are stained with Syto® 59 (red). Scale bar = 20 μm.

dendrimers.¹⁶ No noticeable green fluorescence was observed in the *E. coli* cells treated with a negatively charged, non-targeted dendrimer (GA)G5 which is consistent with the lack of binding in the cell wall SPR model. Thus this imaging study is supportive of a positive correlation between dendrimer adsorption in *E. coli* cells and the LPS cell wall model.

3.4 Antimicrobial activity

Binding to LPS by the dendrimer conjugates likely leads to cell lysis and thus antimicrobial activity in the same way that PMB kills bacteria through its LPS binding and subsequent membrane disruption.^{34, 36, 50} To measure such activity by conjugates **2–6**, we performed a turbidity assay by measuring the optical density (OD) of bacterial cultures treated with the conjugates at 650 nm. A decrease in OD corresponds to an increase in cell lysis.¹⁶ Fig. 5 summarizes the growth inhibition of *E. coli* exposed to standard antibiotics these conjugates. PMB and ciprofloxacin, an inhibitor of DNA gyrase, displayed potent activity with IC₅₀ values of 0.50 μM and 0.074 μM, respectively. Vancomycin, however, shows much lower activity with an IC₅₀ value of 19 μM as expected because of its poor penetration into the peptidoglycan layer of the Gram-negative cell.

Treatment of *E. coli* with PMB-lacking dendrimers (GA)G5, **3** and **5** resulted in no effect or only weak growth inhibition with IC₅₀ values of >80, 22 and 45 μM, respectively. Interestingly, the carbamate-linked dendrimer **4** did not show enhanced activity despite its PMB conjugation. However, two PMB-conjugated dendrimers showed greater inhibition activities: **6** (IC₅₀ = 0.63 μM) and **2** (IC₅₀ = 2.8 μM; 15 μM per PMB). These results suggest that LPS binding is critical but might be insufficient for causing the antimicrobial activity as illustrated by conjugate **5** and in Fig. 5D. It is interesting to note that the amide-linked conjugate **2** (GA)G5(PMB)_{n = 5,4} showed some antimicrobial activity despite its lack of adsorption to a LPS model surface. We further investigated

whether such activity is correlated to PMB valency (n). Three additional conjugates in this series (GA)G5(PMB)_n (n = 2.2, 9.1, 13.5) were investigated for their antibacterial activities using the same turbidity assay as summarized in Fig. S11. The results suggest improvement in the activity as the valency increases but lack of a linear correlation between the valency and activity. Even the highest PMB valency (n = 13.5) displays only a minimal gain in the activity compared to **2**.

In this aspect, conjugation with PMB serves an effective approach for designing bacteria-targeting antimicrobial agents. However, conjugates lacking PMB can be better suited for other applications such as bacterial detection and isolation which require retention of bacterial capture without causing cell rupture. Similar to the SPR study, this assay shows the importance of auxiliary groups on the dendrimer surface. Excess EA branches extended through amine functionality (**6**) cause more potent cell lysis than those through the carbamate (**4**) or carboxylate termini (**2**). However other structural parameters might play a role since variation in hydrodynamic size and conformational flexibility also can contribute to binding and penetration into the actual bacterial cell wall which is much more complex than in the model system⁵¹ primarily due to its high surface charge density, polarity and the exposure of bacterial lipoproteins.

Given the notion that the PAMAM dendrimer NP provides cavities for drug complexation,^{41, 52} we prepared non-covalent

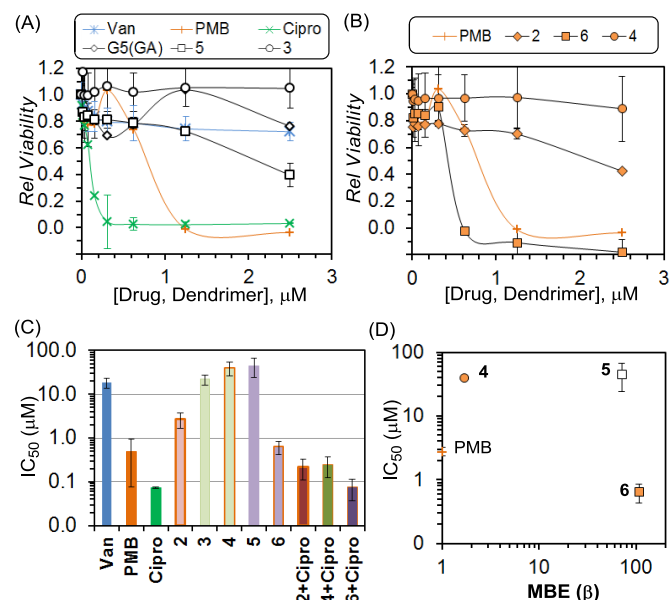


Fig. 5 *In vitro* antibacterial activities of drugs, dendrimers **2–6** and drug mixtures evaluated by a turbidity assay against *E. coli* (XL-1). (A, B) Standard cell viability curves at low μM doses. (C) IC₅₀ values (±SD) of cell viability under various treatments. Each mixture (**2**, **4** or **6** + ciprofloxacin) was made at a 1:1 molar ratio. (D) *In vitro* antibacterial activities (IC₅₀) of conjugate series **4–6** plotted as a function of multivalency binding enhancement (β; Table 1).

complexes of three representative dendrimers **2**, **4**, **6**, each with ciprofloxacin, and tested whether the complex retains the activity of the payload through extended slow release (Fig. S12). Cipro-NP complex formation was confirmed for **2** and **6** and for **4** to a lesser

extent through dialysis diffusion experiments. As shown in Fig. 5C, each complex made at a 1:1 molar ratio showed comparable activity ($IC_{50} \approx 0.25\text{--}0.075 \mu\text{M}$) to free ciprofloxacin. Retention of such antibacterial activity is attributed to the release of drug payload carried by the dendrimer conjugate which is in good agreement with the drug release kinetics determined in a cell-free solution (Fig. S12). The ability to target LPS and carry a payload demonstrates a dual function critically required for the targeted delivery of antimicrobial agents. We believe that identification of these LPS-targeting dendrimer nanocarriers provides an important strategy for extending the half-life of a drug payload and improving its pharmacokinetic distribution and efficacy *in vivo* as supported by numerous studies in polymer-based pharmaceuticals.⁵³ This *in vitro* observation is supportive of the potential application of this nanoplatform for Gram-negative cell targeted drug delivery, which constitutes one of our future research directions.

4 Conclusions

We described the effectiveness of a heteromultivalent strategy for producing high avidity dendrimers for targeting LPS. The G5 PAMAM dendrimer serves as a scaffold uniquely suited for this purpose since its dendritic branches are highly amenable for conjugation with a PMB ligand and also readily modifiable to PMB-mimicking auxiliary residues. A combination of close proximity and dendritic organization of EA amine-based auxiliary ligands is believed to maximize the binding and antimicrobial efficiency of the primary ligand even presented at a low valency ($n_{\text{mean}} \approx 1.2$; $n < 2$ (66%)). This study provides evidence supportive of LPS-binding dendrimers as a multifunctional nanoplatform that serves as an effective potential method for bacterial detection or bacteria-targeted drug delivery. The heteromultivalent strategy presented here may be applicable to other systems in which conjugation of a primary ligand at a low valency is more desired due to intrinsic ligand toxicity like PMB and limited synthetic availability.

Acknowledgements

This study is supported by Michigan Nanotechnology Institute for Medicine and Biological Sciences, and the funding by the University of Michigan Office of the Vice President for Research, and Shanghai Jiao Tong University (SKC).

Notes and references

- D. Liu, ed., *Molecular Detection of Human Bacterial Pathogens*, CRC Press, Boca Raton, FL, 2011.
- S. J. Wagner, L. I. Friedman and R. Y. Dodd, *Clinical Microbiology Reviews*, 1994, **7**, 290-302.
- V. A. Petrenko and I. B. Sorokulova, *J. Microbiol. Methods*, 2004, **58**, 147-168.
- G. A. Jacoby and G. L. Archer, *N. Engl. J. Med.*, 1991, **324**, 601-612.
- H. J. Chung, C. M. Castro, H. Im, H. Lee and R. Weissleder, *Nat. Nanotechnol.*, 2013, **8**, 369-375.
- W. M. Leevy, S. T. Gammon, H. Jiang, J. R. Johnson, D. J. Maxwell, E. N. Jackson, M. Marquez, D. Piwnica-Worms and B. D. Smith, *J. Am. Chem. Soc.*, 2006, **128**, 16476-16477.
- C. Bettegowda, C. A. Foss, I. Cheong, Y. Wang, L. Diaz, N. Agrawal, J. Fox, J. Dick, L. H. Dang, S. Zhou, K. W. Kinzler, B. Vogelstein and M. G. Pomper, *Proc. Natl. Acad. Sci. U. S. A.*, 2005, **102**, 1145-1150.
- H. Gu, P. L. Ho, E. Tong, L. Wang and B. Xu, *Nano Lett.*, 2003, **3**, 1261-1263.
- A. J. Kell, G. Stewart, S. Ryan, R. Peytavi, M. Boissinot, A. Huletsky, M. G. Bergeron and B. Simard, *ACS Nano*, 2008, **2**, 1777-1788.
- H. Gu, P.-L. Ho, K. W. T. Tsang, L. Wang and B. Xu, *J. Am. Chem. Soc.*, 2003, **125**, 15702-15703.
- J.-J. Lee, K. J. Jeong, M. Hashimoto, A. H. Kwon, A. Rwei, S. A. Shankarappa, J. H. Tsui and D. S. Kohane, *Nano Lett.*, 2014, **14**, 1-5.
- P.-C. Lin, C.-C. Yu, H.-T. Wu, Y.-W. Lu, C.-L. Han, A.-K. Su, Y.-J. Chen and C.-C. Lin, *Biomacromolecules*, 2012, **14**, 160-168.
- S. J. Metallo, R. S. Kane, R. E. Holmlin and G. M. Whitesides, *J. Am. Chem. Soc.*, 2003, **125**, 4534-4540.
- V. M. Krishnamurthy, L. J. Quinton, L. A. Estroff, S. J. Metallo, J. M. Isaacs, J. P. Mizgerd and G. M. Whitesides, *Biomaterials*, 2006, **27**, 3663-3674.
- P. Sarker, J. Shepherd, K. Swindells, I. Douglas, S. MacNeil, L. Swanson and S. Rimmer, *Biomacromolecules*, 2010, **12**, 1-5.
- S. K. Choi, A. Myc, J. E. Silpe, M. Sumit, P. T. Wong, K. McCarthy, A. M. Desai, T. P. Thomas, A. Kotlyar, M. M. Banaszak Holl, B. G. Orr and J. R. Baker, *ACS Nano*, 2013, **7**, 214-228.
- J. H. Kang, M. Super, C. W. Yung, R. M. Cooper, K. Domansky, A. R. Graveline, T. Mammoto, J. B. Berthet, H. Tobin, M. J. Cartwright, A. L. Watters, M. Rottman, A. Waterhouse, A. Mammoto, N. Gamini, M. J. Rodas, A. Kole, A. Jiang, T. M. Valentin, A. Diaz, K. Takahashi and D. E. Ingber, *Nat. Med. (N. Y., NY, U. S.)*, 2014, **20**, 1211-1216.
- G. A. Johnson, N. Muthukrishnan and J.-P. Pellois, *Bioconjugate Chem.*, 2012, **24**, 114-123.
- G. A. Johnson, E. A. Ellis, H. Kim, N. Muthukrishnan, T. Snavelly and J.-P. Pellois, *PLoS ONE*, 2014, **9**, e91220.
- L. L. Kiessling, J. E. Gestwicki and L. E. Strong, *Angew. Chem. Int. Ed.*, 2006, **45**, 2348-2368.
- M. Mammen, S. K. Choi and G. M. Whitesides, *Angew. Chem., Int. Ed.*, 1998, **37**, 2754-2794.
- C. Fasting, C. A. Schalley, M. Weber, O. Seitz, S. Hecht, B. Kokschi, J. Dervede, C. Graf, E.-W. Knapp and R. Haag, *Angew. Chem. Intl. Ed.*, 2012, **51**, 10472-10498.
- C. Walsh, *Nature (London, U.K.)*, 2000, **406**, 775-781.
- J. Rao and G. M. Whitesides, *J. Am. Chem. Soc.*, 1997, **119**, 10286-10290.
- H. J. Chung, T. Reiner, G. Budin, C. Min, M. Liong, D. Issadore, H. Lee and R. Weissleder, *ACS Nano*, 2011, **5**, 8834-8841.
- G. Birkenmeier, S. Nicklisch, C. Pockelt, A. Mossie, V. Steger, C. Gläser, S. Hauschildt, E. Usbeck, K. Huse, U. Sack, M. Bauer and A. Schäfer, *J. Pharmacol. Exp. Ther.*, 2006, **318**, 762-771.
- J. J. Drabick, A. K. Bhattacharjee, D. L. Hoover, G. E. Siber, V. E. Morales, L. D. Young, S. L. Brown and A. S. Cross, *Antimicrob. Agents Chemother.*, 1998, **42**, 583-588.
- L. Xu, J. S. Josan, J. Vagner, M. R. Caplan, V. J. Hruby, E. A. Mash, R. M. Lynch, D. L. Morse and R. J. Gillies, *Proc. Natl. Acad. Sci. U. S. A.*, 2012, **109**, 21295-21300.
- H. Zhou, P. Jiao, L. Yang, X. Li and B. Yan, *J. Am. Chem. Soc.*, 2010, **133**, 680-682.
- S.-K. Choi, M. Mammen and G. M. Whitesides, *J. Am. Chem. Soc.*, 1997, **119**, 4103-4111.
- D. Ponader, P. Maffre, J. Aretz, D. Pussak, N. M. Ninnemann, S. Schmidt, P. H. Seeberger, C. Rademacher, G. U. Nienhaus and L. Hartmann, *J. Am. Chem. Soc.*, 2014, **136**, 2008-2016.
- P. F. Mühlradt, J. Menzel, J. R. Golecki and V. Speth, *Eur. J. Biochem.*, 1974, **43**, 533-539.
- T. Velkov, P. E. Thompson, R. L. Nation and J. Li, *J. Med. Chem.*, 2009, **53**, 1898-1916.
- J. Mares, S. Kumaran, M. Gobbo and O. Zerbe, *J. Biol. Chem.*, 2009, **284**, 11498-11506.
- N. Yin, R. L. Marshall, S. Matheson and P. B. Savage, *J. Am. Chem. Soc.*, 2003, **125**, 2426-2435.
- R. A. Moore, N. C. Bates and R. E. Hancock, *Antimicrob. Agents Chemother.*, 1986, **29**, 496-500.
- C. J. Thomas and A. Surolija, *FEBS Lett.*, 1999, **445**, 420-424.
- K. Abdelraouf, K. H. Braggas, T. Yin, L. D. Truong, M. Hu and V. H. Tam, *Antimicrob. Agents Chemother.*, 2012, **56**, 4625-4629.
- S. K. Choi, P. Leroueil, M.-H. Li, A. Desai, H. Zong, A. F. L. Van Der Spek and J. R. Baker Jr, *Macromolecules*, 2011, **44**, 4026-4029.

- 40 S. K. Choi, T. Thomas, M. Li, A. Kotlyar, A. Desai and J. R. Baker Jr, *Chem. Commun. (Cambridge, U. K.)*, 2010, **46**, 2632–2634.
- 41 S. K. Choi, T. P. Thomas, P. R. Leroueil, A. Kotlyar, A. F. L. Van Der Spek and J. R. Baker, *J. Phys. Chem. B*, 2012, **116**, 10387–10397.
- 42 P. T. Wong, S. H. Wang, S. Ciotti, P. E. Makidon, D. M. Smith, Y. Fan, C. F. Schuler and J. R. Baker, *Mol. Pharmaceutics*, 2014, **11**, 531–544.
- 43 P. T. Wong, K. Tang, A. Coulter, S. Tang, J. R. Baker and S. K. Choi, *Biomacromolecules*, 2014, **15**, 4134–4145.
- 44 M.-H. Li, S. K. Choi, P. Leroueil and J. R. Baker, *ACS Nano*, 2014, **8**, 5600–5609.
- 45 J. E. Silpe, M. Sumit, T. P. Thomas, B. Huang, A. Kotlyar, M. A. van Dongen, M. M. Banaszak Holl, B. G. Orr and S. K. Choi, *ACS Chem. Biol.*, 2013, **8**, 2063–2071.
- 46 N. J. de Mol and M. J. E. Fischer, in *Handbook of Surface Plasmon Resonance*, The Royal Society of Chemistry, 2008, pp. 123–172.
- 47 S. Bharathi, P. T. Wong, A. Desai, O. Lykhyska, V. Choe, H. Kim, T. P. Thomas, J. R. Baker and S. K. Choi, *J. Mater. Chem. B*, 2014, **2**, 1068–1078.
- 48 A. B. Witte, A. N. Leistra, P. T. Wong, S. Bharathi, K. Refior, P. Smith, O. Kaso, K. Sinniah and S. K. Choi, *J. Phys. Chem. B*, 2014, **118**, 2872–2882.
- 49 D. A. Tomalia, A. M. Naylor and I. William A. Goddard, *Angew. Chem., Int. Ed.*, 1990, **29**, 138–175.
- 50 Z. Z. Deris, J. D. Swarbrick, K. D. Roberts, M. A. K. Azad, J. Akter, A. S. Horne, R. L. Nation, K. L. Rogers, P. E. Thompson, T. Velkov and J. Li, *Bioconjugate Chem.*, 2014, **25**, 750–760.
- 51 M. K. Calabretta, A. Kumar, A. M. McDermott and C. Cai, *Biomacromolecules*, 2007, **8**, 1807–1811.
- 52 J. Hu, T. Xu and Y. Cheng, *Chem. Rev. (Washington, DC, U. S.)*, 2012, **112**, 3856–3891.
- 53 M. J. Vicent, H. Ringsdorf and R. Duncan, *Adv. Drug Delivery Rev.*, 2009, **61**, 1117–1120.

Table of Contents Graphic

Heteromultivalent design of PAMAM dendrimer by conjugation with polymyxin B (PMB) ligand and excess auxiliary ethanolamine (EA) branches led to lipopolysaccharide (LPS) avidity two orders of magnitude greater than free PMB.

